EFFECT OF TEMPERATURE ON ULTIMATE CAPACITY OF LINED CONTAINMENT UNDER SEVERE ACCIDENT CONDITIONS

Ajai S Pisharady[1], Sourav Acharya[1], L R Bishnoi[1]

[1] Siting & Structural Engineering Division, AERB, Mumbai, India (aspisharady@aerb.gov.in)

ABSTRACT

Containment structure is the most important civil engineering structure of a nuclear power plant (NPP), housing the reactor and major safety related components. Evaluation of ultimate load capacity (ULC) of containment is carried out to establish pressure resistance margin over its design pressure. To gain confidence in analytical predictions, analysis methodology and models are validated by comparing with the experimental results for pressure loading on scaled model of containment. This paper brings out salient aspects of analytical calculations for evaluating ultimate load capacity of prestressed concrete containment vessel (PCCV) undertaken as AERB-USNRC Standard problem Exercise - 3 (SPE-3). One of the objectives of this SPE was to investigate the effect of temperature on ultimate load capacity of containment. Comparison of ULC of PCCV with and without temperature is carried out in the paper. Two simulated severe accident conditions are considered. It is noted that the ULC reduces in presence of temperature loading.

INTRODUCTION

Containment structure is the most important civil engineering structure of a nuclear power plant (NPP), housing the reactor and major safety related components. It is the final barrier against release of radioactivity to environment. Containment structures are designed to resist, within the elastic range of material stress, the pressure due to design basis accident. Containment design requirements include assurance of structural integrity and specified leak tightness. Containment structures are mostly pre-stressed concrete structures, with or without a steel liner. For lined containments, the leak tightness requirement is served by the steel liner.

Evaluation of ultimate load capacity (ULC) of containment is carried out to establish pressure resistance margin over its design pressure. ULC is calculated by analytical approaches considering realistic behaviour of materials, unlike the conservative elastic behaviour assumed in design stage. To gain confidence in analytical predictions, analysis methodology and models are validated through experiments on scaled model of containments. The AERB-USNRC Standard problem Exercise - 3 (SPE-3) on "Performance of Containment Vessel Under Severe Accident Conditions" was framed on the basis of 1:4-Scale pre-stressed concrete containment vessel (PCCV) model tests performed at Sandia National Laboratory, USA. Scope of the exercise included analytical assessment of ultimate load capacity of PCCV and characterization of its leakage behaviour as a function of pressure and temperature.

In any accident scenario, the containment is subjected to simultaneous action of pressure and temperature. ULC studies reported so far have generally ignored the effect of temperature, Mathet et al. (2005). One of the objectives of this SPE was to investigate the effect of temperature on ultimate load capacity of containment. This paper discusses the ULC analysis of PCCV with and without temperature. Two simulated severe accident conditions were considered: first corresponding to saturated steam pseudo-time history; and second corresponding to station black-out time history. Results from all three analyses have been compared at selected containment locations.

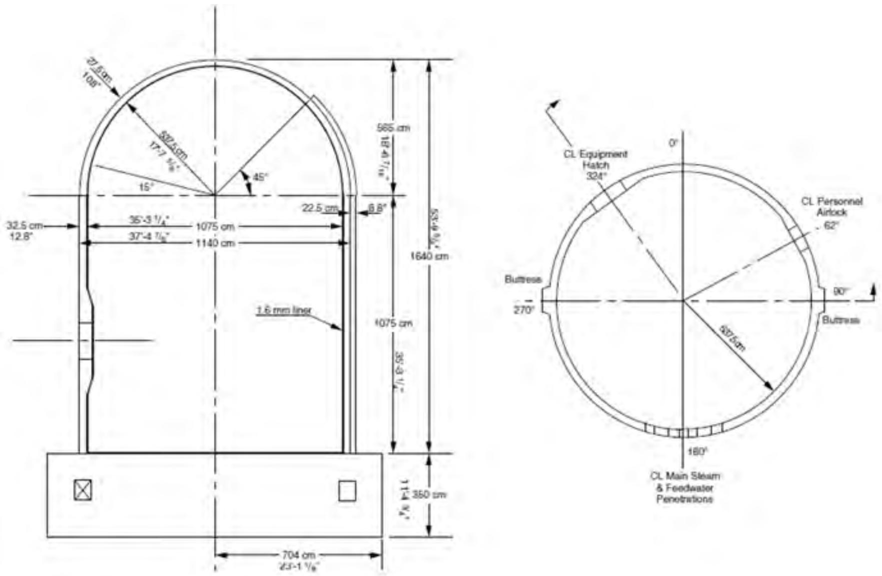

Figure 1 . Geometric details of the prestressed concrete containment test vessel, Hessheimer et al. (2003)

PCCV TEST MODEL DESCRIPTION

The PCCV test model was a pre-stressed concrete cylinder of 10.8m diameter with wall thickness of 325mm, a 3500mm thick base mat and a hemispherical dome of thickness 275mm, all constructed with a nominal concrete strength of 45 MPa. The pre-stressing was accomplished with hairpin shaped meridional tendons and circular hoop tendons. The meridional tendons were anchored in stressing gallery. The anchorages of the hoop tendons were staggered in the buttresses located at 90^o and 270^o azimuths. Two major openings in the cylinder represents opening for equipment hatch and airlock. Figure - 1 depicts geometric details of the PCCV test model, Hessheimer et al. (2003).

Finite Element Model

The finite element model of the PCCV was developed in ABAQUS using 4-node quadrilateral layered shell element with reduced integration. Large-strain formulation was used for the study. Centreline modelling was adopted for modelling the concrete sections. The gross cross section is modelled as two layers; layer - 1: liner having nine integration points along its thickness and layer - 2 to 4: concrete-steel composite, each having nine integration points along the thickness. Figure 2 depicts finite element model of PCCV. Only two major openings are considered in the present model as follows:

1. The equipment hatch: Diameter 1.54m, at 324^o and elevation of centre at 4.675m
2. The airlock: Diameter 0.661m, at 62^o and elevation of centre at 4.525m.

The PCCV concrete is reinforced with two layers of hoop and meridional steel at inner and outer faces. These reinforcements are simulated as smeared steel layers with thickness equal to the ratio of the rebar area to the rebar spacing. Pre-stressing tendons are also modelled as smeared steel layers. The structure is assumed fixed at the top of base mat. Hence the base mat has not been included in the finite element model.

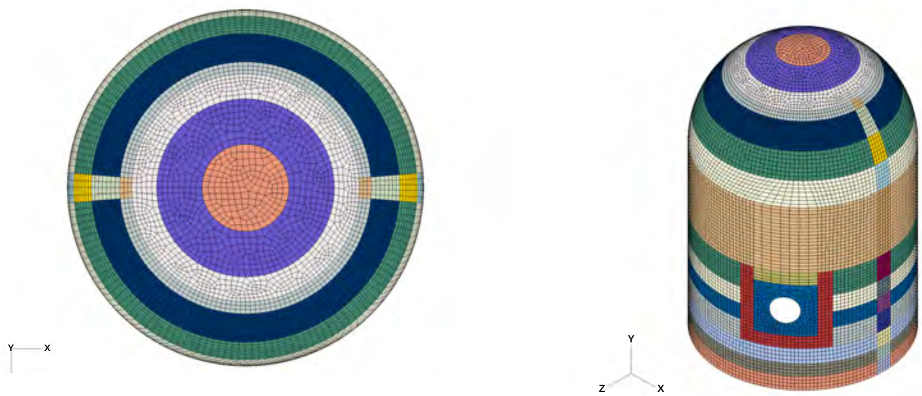

Figure 2 . Finite element model of the pre-stressed concrete containment test vessel

Material Constitutive Models

The concrete damage plasticity model available in ABAQUS is used to model the non-linear behaviour of concrete, ABAQUS-610 (2010). The main failure mechanisms assumed in the model are tensile cracking and compressive crushing of the concrete material. The failure surface is controlled by two variables representing the equivalent plastic strains in compression and tension. In the current study, the damage variables are not specified. This leads the damage plasticity model behaving as the plasticity model only.

The steel behaviour is represented by metal plasticity models available in ABAQUS with yield stress of 390 MPa for passive reinforcement, 1590 MPa for prestress steel and 375 MPa for liner steel. Effects associated with rebar/concrete interface, such as bond slip and dowel action are simulated by concrete tension stiffening model allowing load transfer across cracks through the rebar until bond failure.

Loading

Pre-stress is introduced as an initial stress. Variation of pre-stress along the length of cables and effect of deviation of cables around the openings are not included. The applied pre-stress is based on calculated average value along the cable length based on the prestress data given in Hessheimer et al. (2003). The adopted average values are

- Hoop cables: 840 x $10^6 N/m^2$
- Hairpin cables in cylinder and dome region up to the height of buttress: 1250 x $10^6 N/m^2$
- Hairpin cables in dome region above the buttress height: 1000 x $10^6 N/m^2$

Variation of temperature across the thickness at different time steps is provided in the problem definition for case-1 and case-2 in terms of discrete temperature values at 25 points across the thickness, AERB-USNRC (2011). In both cases the stress free temperature has been assumed to be $25^o C$. This value is kept constant across the thickness and applied as an initial condition using the predefined field definition available in ABAQUS. Further variation at each time step has been applied by dividing the model into five temperature regime as indicated in figure 3. For each time step, the temperature across concrete section was approximated as piece-wise linear along 25 equally spaced points within the section. Figure 4 illustrates typical difference between the actual distribution and modelled distribution in temperature regime-1 (see figure 3) for case - 1 and case - 2.

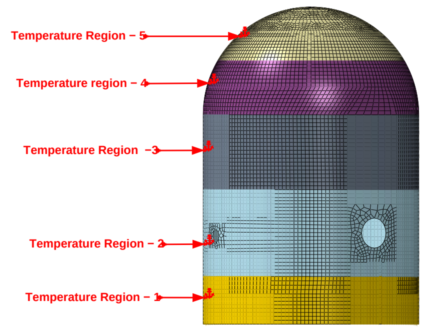

Figure 3 . Different temperature regime over the containment geometry

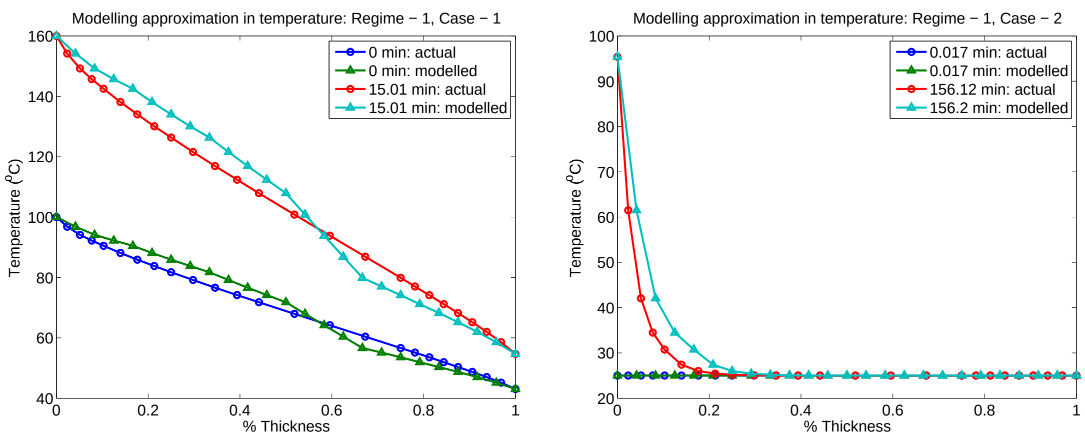

Figure 4 . Typical variation of temperature distribution across thickness for case 1 and 2

Internal pressure was applied in incremental static load steps. Since penetrations for equipment hatch and airlock openings are not modelled exclusively, the equivalent pressure forces at these openings were applied as distributed nodal forces along the periphery of these openings. Initial condition of the structure before application of pressure was the one obtained after application of pre-stress and then the initial temperature at zero pressure. The load steps were increased so as to realistically capture the increase in temperature and pressure as indicated in figures 5 and 6,AERB-USNRC (2011).

The effect of dilation of pre-stressing cables, which in turn is expected to induce some additional pre-stress is not modelled. The inclusion of this effect may result in some increase of the ultimate capacity of the structure over the one determined using the current computational model.

Failure Prediction Criteria

The containment vessel was considered to have reached its ultimate structural failure capacity when yielding of reinforcing steel as well as pre-stressing steel in all directions occur in any location in the structure, leading to general yield condition in the region, Pisharady et al. (2012).

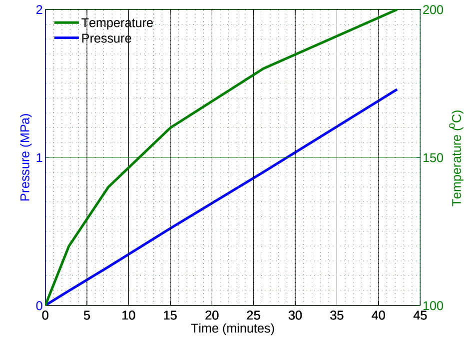

Figure 5 . Temperature and pressure: Case - 1

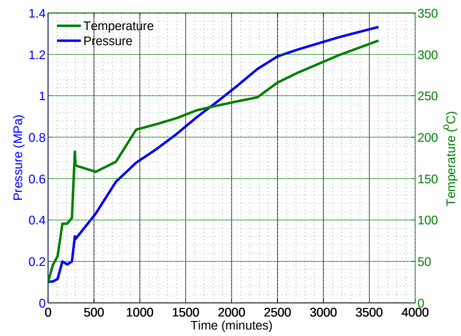

Figure 6 . Temperature and pressure: Case - 2

ULC ANALYSIS OF PCCV

ULC analysis of PCCV was carried out, and results in terms of displacements, strains and stresses were retrieved at important locations for three cases:

1. Case - 0: Linear increase in pressure without temperature
2. Case - 1: Temperature and pressure variation corresponding to a postulated saturated steam pseudo-time history (figure 5)
3. Case - 2; Temperature and pressure corresponding to a postulated station black-out time history (figure 6)

Material degradation due to temperature is not considered, as the effect of this is considered to be minimal. For case - 2, analysis with loading corresponding to saturated steam pseudo-time history, it was noticed that at zero pressure, the temperature is higher than the stress free temperature at the inner face. This induced strains and deformation at zero pressure, which was accounted.

RESULTS

Failure Location, Stress Distribution and Deformed Shapes

Failure initiated adjacent to the equipment hatch opening, mainly in the region between equipment hatch and airlock in all the three cases. Calculated ultimate pressure capacities of PCCV for the three cases are given in table 1. The stress distribution in hoop and meridional pre-stress cable layers at ultimate pressure for all three cases is shown in figure 7. The calculated ULC (structural collapse) of 3.65 P_d and the failure location for pressure loading (case-0) compares very well with the reported results, Hessheimer et al. (2003).

Deformed shapes of the PCCV at various pressure stages for case - 0 analysis are shown in figure 8. Plots of pressure vs deformation at dome crown, general area of cylinder, location near equipment hatch and location near air lock for all the three analysed cases are shown in figure 9.

Tendon Stress Profile

Individual pre-stressing tendons were not modelled in the present analysis. However to understand the distribution of tendon stress across the length, at different pressure, stress in pre-stressing cable layer

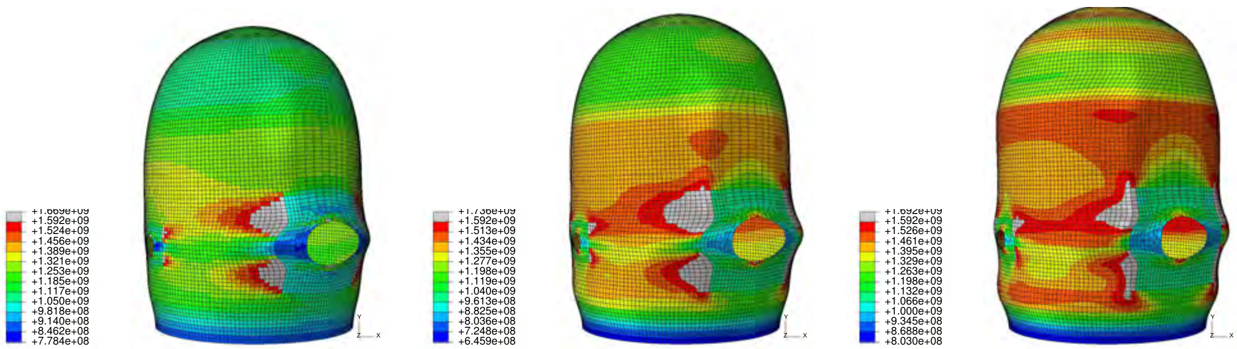

Case - 0 Case - 1 Case - 2

Hoop cables

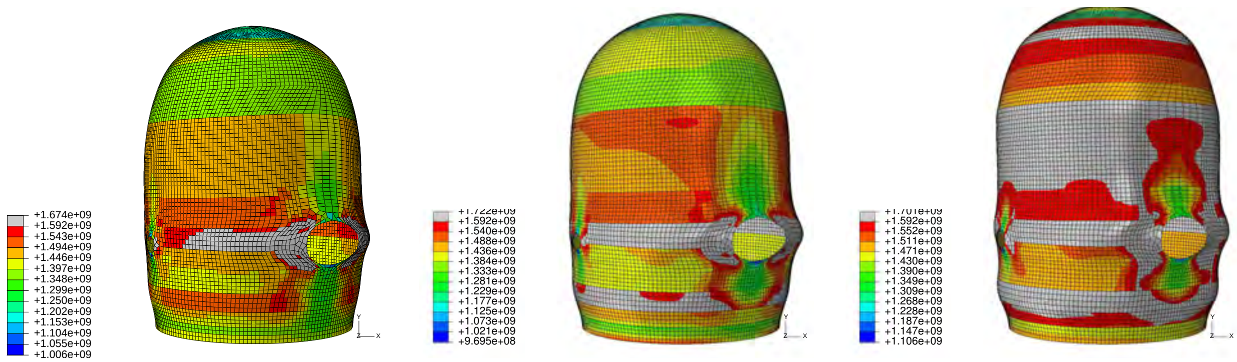

Case - 0 Case - 1 Case - 2

Meridional cables

Figure 7 . Stresses in prestress cable layers at ultimate pressure

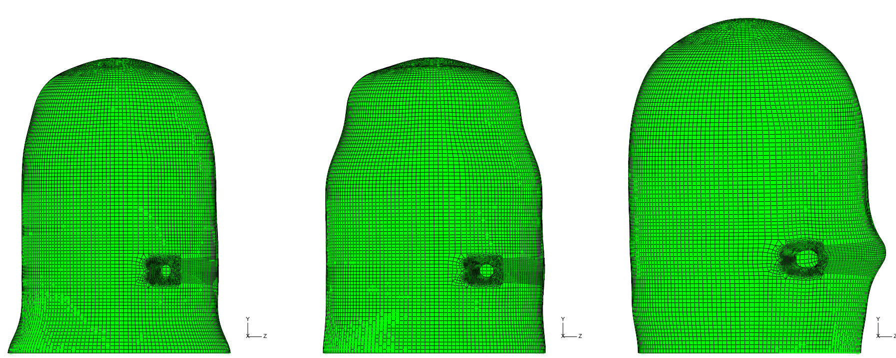

After prestress Pressure = $1.00P_d$ Pressure = $3.65P_d$

Figure 8 . Deformed shape of PCCV at different pressure stages

Table 1 : Ultimate load capacity of PCCV under different conditions

Study	Loading	Ultimate capacity
Case - 0	Internal pressure	3.65 P_d
Case - 1	Internal pressure & temperature (Saturated steam pseudo time history)	3.46 P_d
Case - 2	Internal pressure & temperature (SBO time history)	3.3 P_d

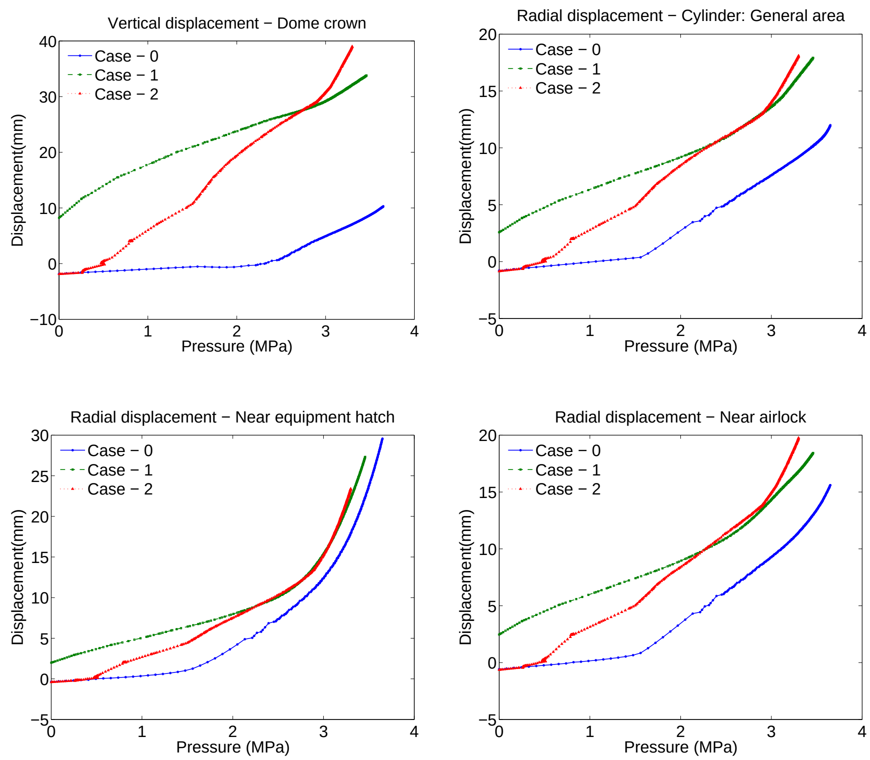

Figure 9 . Comparison of displacements at selected locations

at the level of the tendon along its path has been extracted. Tendon stress distribution for a typical tendon (H68) for different pressure stages of all the three analysed cases is plotted in figure 10.

SUMMARY

1. Global model of PCCV was developed to evaluate its ultimate pressure capacity. A special technique was adopted to simulate temperature variation across wall section in the study. The PCCV cross section is modeled using layered shell elements and reinforcement is included as an embedded oriented surface inside the shell. Effect of tendon slippage and liner-concrete interaction are not included.

2. Failure is initiated adjacent to the equipment hatch opening, mainly in the region between equipment hatch and airlock in all three analysed cases. The predicted failure pressure and failure location for pressure loading case match closely with the reported test results.

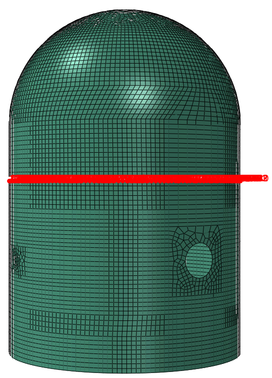

Path of H-68 tendon

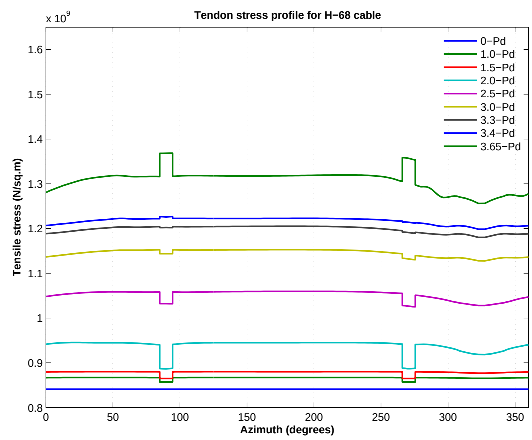

Case - 0

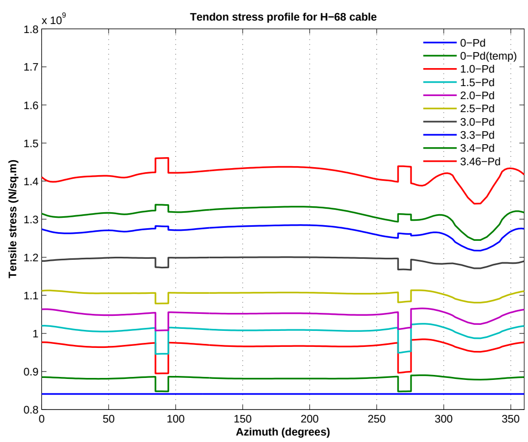

Case - 1

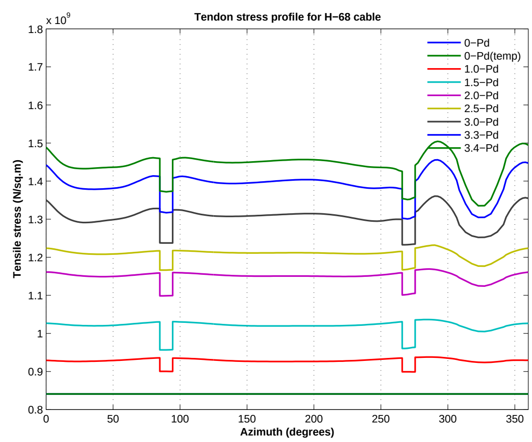

Case - 2

Figure 10 . Tendon stress profile for H-68 tendon

3. Limitations of the current study:
    - Variation of tendon force along its length could not be included.
    - As pre-stress tendons were not modelled individually, stress variation in tendons could not be captured exactly.
    - Degradation of material properties with temperature was not considered.
4. Comparison of the ultimate pressure capacity of the PCCV for the three analysed cases indicates that the ULC decreases in presence of temperature. However, the location of failure remains almost the same.

REFERENCES

ABAQUS-610 (2010), “ABAQUS 6.10 User Documentation - Theory manual”, Dassault Systems Simulia Corp., Providence, RI, USA, 2010.

AERB-USNRC (2011), “White paper to define phase - 2 analysis of SPE - 3 on Performance of containment vessel under severe accident conditions”, Technical report, USNRC, Washington, USA.

Hessheimer, M. F., Klamerus, E. W., Lambert, L. D., Rightley, G. S. & Dameron, R. A. (2003), “overpressurization test of a 1:4-scale prestressed concrete containment vessel model”, Technical report NUREG/CR-6810; SAND2003-0840P, Sandia National Laboratories and USNRC, USA, Washington, USA.

Mathet, E., Hessheimer, M. & Dameron, R. (2005), “Final report on International Standard Problem No. 48 Containment Capacity”, Technical report, NEA/CSNI.

Pisharady, A. S., Acharya, S. & Bishnoi, L. R. (2012), “final report of phase - 2 analysis for Standard Problem Exercise - 3 on performance of containment vessel under severe accident conditions”, Technical report, Atomic Energy Regulatory Board, Mumbai, India.